Recombinant Human Thioredoxin-1 Protects Macrophages from Oxidized Low-Density Lipoprotein-Induced Foam Cell Formation and Cell Apoptosis

Hui Zhang, Qi Liu, Jia-Le Lin, Yu Wang, Ruo-Xi Zhang, Jing-Bo Hou* and Bo Yu

Department of Cardiology, Key Laboratories of Education Ministry for Myocardial Ischemia Mechanism and Treatment, the Second Affiliated Hospital of Harbin Medical University, Harbin 150086, China

Abstract

Oxidized low-density lipoprotein (ox-LDL)-induced macrophage foam cell formation and apoptosis play critical roles in the pathogenesis of atherosclerosis. Thioredoxin-1 (Trx) is an antioxidant that potently protects various cells from oxidative stress-induced cell death. However, the protective effect of Trx on ox-LDL-induced macrophage foam cell formation and apoptosis has not been studied. This study aims to investigate the effect of recombinant human Trx (rhTrx) on ox-LDL-stimulated RAW264.7 macrophages and elucidate the possible mechanisms. RhTrx significantly inhibited ox-LDL-induced cholesterol accumulation and apoptosis in RAW264.7 macrophages. RhTrx also suppressed the ox-LDL-induced overproduction of lectin-like oxidized LDL receptor (LOX-1), Bax and activated caspase-3, but it increased the expression of Bcl-2. In addition, rhTrx markedly inhibited the ox-LDL-induced production of intracellular reactive oxygen species (ROS) and phosphorylation of p38 mitogen-activated protein kinases (MAPK). Furthermore, anisomycin (a p38 MAPK activator) abolished the protective effect of rhTrx on ox-LDL-stimulated RAW264.7 cells, and SB203580 (a p38 MAPK inhibitor) exerted a similar effect as rhTrx. Collectively, these findings indicate that rhTrx suppresses ox-LDL-stimulated foam cell formation and macrophage apoptosis by inhibiting ROS generation, p38 MAPK activation and LOX-1 expression. Therefore, we propose that rhTrx has therapeutic potential in the prevention and treatment of atherosclerosis.

Key Words: Thioredoxin-1, Foam cell, Apoptosis, Atherosclerosis, p38 MAPK

INTRODUCTION

Atherosclerosis is the most common type of cardiovascular disease and is currently the leading cause of mortality worldwide (Gleissner, 2016). Macrophage foam cell formation (Lin *et al*., 2015) and apoptosis (Tabas, 2009) are key mediators in the pathogenesis of atherosclerosis. Many experiments have shown that in the lesional area, macrophage apoptosis participates in the formation and expansion of the lipid core and leads to inflammation and necrosis, both of which result in plaque instability, plaque rupture and myocardial infarction (Liao *et al*., 2012; Moore *et al*., 2013; Dai *et al*., 2014). Therefore, protecting macrophages from foam cell formation and apoptosis is considered an effective therapeutic strategy to attenuate plaque instability and combat acute vascular events.

In the pathogenesis of atherosclerosis, macrophages take up ox-LDL via several scavenger receptors (SRs), such as SR-AI, SR-BI, CD36 and lectin-like oxidized LDL receptor (LOX-1) (Pirillo *et al*., 2013). Ox-LDL uptake by SRs induces the generation of reactive oxygen species (ROS) and phosphorylation of p38 mitogen-activated protein kinases (MAPK). Activated p38 MAPK subsequently activates or inactivates specific downstream effectors by phosphorylation to induce cellular responses to the stimuli (Cuadrado and Nebreda, 2010). The phosphorylation of p38 MAPK up-regulates the expression of LOX-1, increasing the uptake of ox-LDL and promoting foam cell formation (Ishiyama *et al*., 2010). Apoptosis is another important outcome of p38 MAPK activation. Activation of p38 MAPK induces apoptotic pathways primarily by promoting the transcription of pro-apoptotic genes and regulating the activity of apoptosis-related Bcl-2 family proteins, such as Bcl-2 and Bax (Cuadrado and Nebreda, 2010), resulting in the activation of caspase-3 and cell apoptosis.

Thioredoxin (Trx), a small ubiquitous thiol protein (12 kDa),

www.biomolther.org

was originally identified as a hydrogen donor for ribonucleotide reductase in *Escherichia coli* (Laurent *et al*., 1964). It interacts with oxidized cysteine groups in proteins through its highly conserved active site, Cys-Gly-Pro-Cys. Once oxidized, Trx is reduced by thioredoxin reductase (TrxR) (Holmgren, 1985) and nicotinamide adenine dinucleotide phosphate (NADPH) (Powis and Montfort, 2001). Thus, Trx is believed to be a potent scavenger of ROS. Additionally, Trx has multiple functions, including antioxidant (D'Annunzio *et al*., 2016), anti-inflammatory (Chen *et al*., 2016), and anti-apoptotic (Kamimoto *et al*., 2010) activities. The administration of recombinant human Trx (rhTrx) was recently shown to attenuate several diseases associated with oxidant-induced apoptosis, including ischemia/reperfusion-induced myocardial damage (Tao *et al*., 2006), transient focal cerebral ischemia (Wang *et al*., 2015) and ethanol-induced liver injury (Cohen *et al*., 2009). Although the molecular mechanisms of these functions are complex and have not been fully elucidated, the cellular activity of Trx likely involves specific signaling cascades. For example, under conditions of oxidative stress, Trx interacts with apoptosis signal-regulating kinase (ASK) 1, a mitogen-activated protein kinase kinase kinase (MKKK) in the p38 MAPK signaling cascade, and prevents it from activating p38 MAPK, thereby negatively regulating apoptosis (Saitoh *et al*., 1998). However, the effect of rhTrx on macrophage exposure to ox-LDL *In vitro* is still unknown.

Therefore, the present study aimed to determine if treatment with rhTrx attenuated ox-LDL-induced foam cell formation and apoptosis in macrophages and to investigate the signaling mechanism underlying the cytoprotective effect of rhTrx against ox-LDL.

MATERIALS AND METHODS

Materials and reagents

The RAW264.7 macrophage cell line was purchased from the Institute of Biochemistry and Cell Biology (Shanghai Institute for Biological Science, the Chinese Academy of Sciences, Shanghai, China). DMEM and fetal bovine serum (FBS) were purchased from HyClone (Logan, UT, USA). RhTrx was purchased from R&D Systems (Minneapolis, MN). Ox-LDL, oil red O, hematoxylin, DMSO and a protease inhibitor cocktail were purchased from Sigma (St. Louis, MO, USA). FITC Annexin V Apoptosis Detection Kit I was purchased from Becton Dickinson (Franklin Lakes, NJ, USA). SB203580 and anisomycin were purchased from Cell Signaling Technology (Danvers, MA, USA). Rabbit monoclonal antibodies against p38 MAPK, p-p38 MAPK, Bcl-2, Bax, and cleaved caspase-3 and goat anti-rabbit IgG HRP-conjugated antibody were purchased from Cell Signaling Technology (Danvers, MA, USA). Rabbit monoclonal antibody against LOX-1 and goat anti-rabbit IgG (H+L) TRITC-conjugated antibody were purchased from Abcam (Cambridge, MA, USA). A ROS Assay Kit was purchased from Beyotime Biotech (Shanghai, China).

Cell culture and treatment

RAW264.7 macrophages were cultured in DMEM supplemented with 10% FBS, penicillin (100 U/mL) and streptomycin (100 μg/mL) at 37°C in a humidified atmosphere with 5% CO_2. The culture medium was replaced every 2-3 days. The rhTrx powder was dissolved in sterile phosphate-buffered

saline (PBS) at a concentration of 1000 μg/mL according to the manufacturer's instructions and stored at -20°C for the subsequent experiments. For ox-LDL treatment, cells at 85%-90% confluence were exposure to ox-LDL (100 mg/L) for 24 h. Cells were preincubated with rhTrx (0, 1, 2, 4 μg/mL) for 20 min before ox-LDL exposure to study the effects of rhTrx. For further analysis of the effects of rhTrx on the phosphorylation of p38 MAPK, cells were treated with a p38 MAPK inhibitor (SB203580; 10 μM) and activator (anisomycin; 25 μg/mL). The inhibitor/activator was added 30 min before ox-LDL. In rhTrx and activator co-treatment experiments, cells were preincubated with the activator for 30 min and then treated with rhTrx before ox-LDL exposure.

Oil red O staining

Cells were pretreated with rhTrx (0, 1, 2, 4 μg/mL) for 20 min before ox-LDL (100 mg/L) exposure. After the previous treatment, the culture medium was removed, and cells were washed three times with PBS and fixed in 4% paraformaldehyde for 20 min. Fixed cells were rinsed with PBS and then with 60% isopropanol for 5 min and then stained with freshly prepared oil red O working solution for 30 min at room temperature. The nuclei were lightly stained with hematoxylin for 5 min. Stained cells were rinsed with distilled water, mounted in glycerine jelly, and then observed using phase-contrast microscopy (IX71; Olympus, Tokyo, Japan).

Cholesterol content

Cells were treated as described above. The lipid contents, including total cholesterol (TC) and free cholesterol (FC), of the treated RAW264.7 cells were measured by enzymatic assay kits according to the protocol from the manufacturer (Abcam). Conjugated cholesterol is calculated as cholesteryl ester (CE) with the following formula: CE=TC-FC.

Apoptosis assays

Apoptosis was analyzed using the FITC Annexin V Apoptosis Detection Kit I (Becton Dickinson) according to the manufacturer's instructions. Cells were treated using the method described above. After treatment, cells were harvested with trypsin (Beyotime Biotech.) and washed twice with cold PBS. Then, the cells were resuspended in 100 μL of binding buffer at a concentration of 1× 10^6 cells/mL. Five microliters each of propidium iodide (PI) and annexin V were added to the cell suspension and incubated at room temperature for 15 min in the dark with gentle vortexing for double staining. Then, the cell suspension was mixed with 400 μL of binding buffer and immediately analyzed using fluorescence-activated cell sorting (FACS) on a flow cytometer (BD Biosciences, San Diego, CA). The number of apoptotic cells was quantified by collecting 10,000 events. The data were analyzed using FlowJo (version 7.6) flow cytometry analysis software (FlowJo LLC, Ashland, OR, USA). All the samples were assayed in triplicate.

Detection of ROS

RAW264.7 cells were incubated with ox-LDL (100 mg/L) for 2 h after a pre-treatment with rhTrx (0, 1, 2, and 4 μg/mL). Cells were washed twice with PBS and then incubated with 10 mM 2',7'-dichlorfluorescein-diacetate (DCFH-DA; Beyotime Institute of Biotechnology, Beijing, China) at 37°C for 15 min. After the cells were washed with serum-free culture medium, DCF fluorescence was detected using a fluorescence micro-
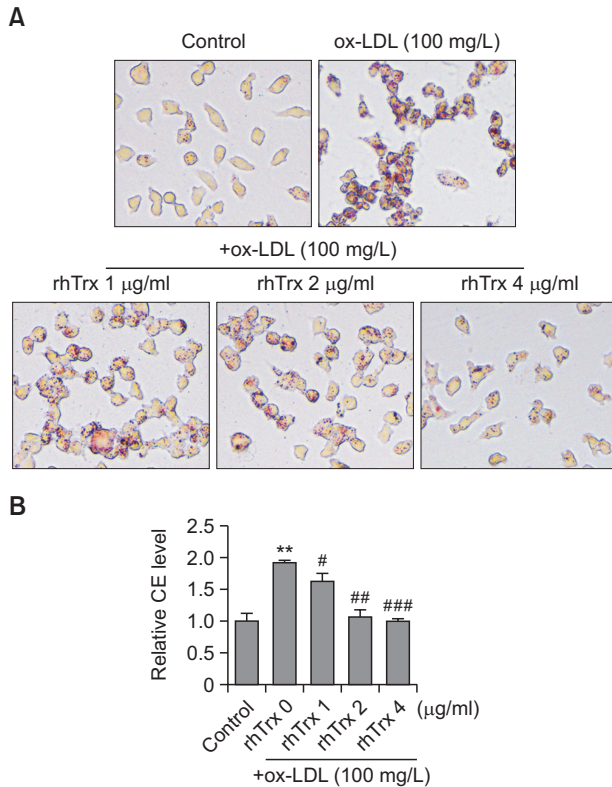
A

B

Fig. 1. RhTrx reduces ox-LDL-induced foam cell formation in RAW264.7 cells. (A) Representative photographs of RAW264.7 cells (oil red O staining, ×200). RAW264.7 cells were incubated with ox-LDL (100 mg/L) for 24 h after pretreatment with rhTrx (0, 1, 2, 4 μg/mL). The red color indicates the stained lipid droplet. (B) Relative levels of CE in RAW264.7 cells. The treatment is the same as in (A). The CE measurements are described in the Materials and Methods section. Values are expressed as the mean ± SD from triplicate experiments. **$p<0.01$ indicates significant differences from the control group, #$p<0.05$, ##$p<0.01$ and ###$p<0.001$ indicate significant differences from the ox-LDL 100 mg/L group.
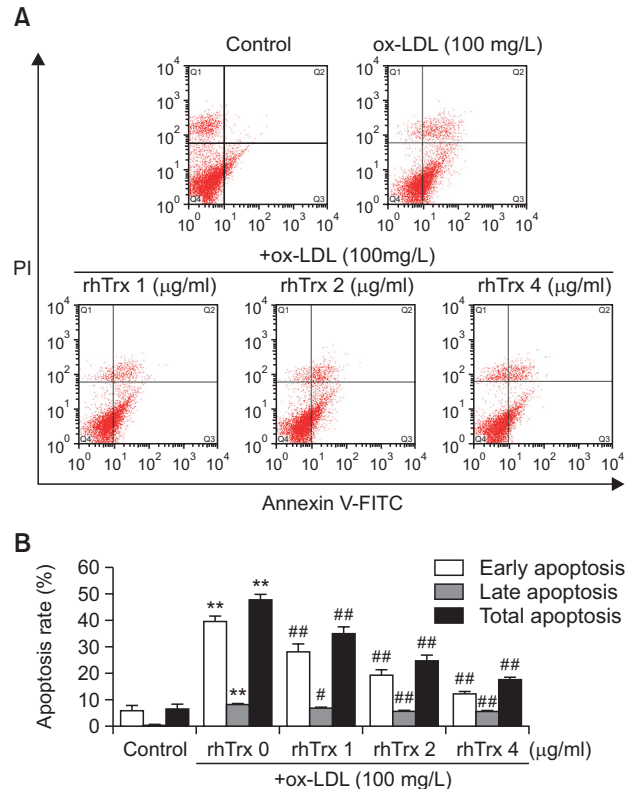
A

B

Fig. 2. RhTrx inhibits ox-LDL-induced cell apoptosis in RAW264.7 cells. Cells were treated as described in Fig. 1. Then, they were stained with annexin V and PI and analyzed using flow cytometry. (A) The apoptosis of RAW264.7 cells is shown by flow cytometry dot plots. The intensity of the PI staining(y-axis) is plotted against the intensity of the annexin V staining (x-axis). In each figure, the upper left (quadrant 1, annexin V-/PI+) represents necrotic cells, the upper right (quadrant 2, annexin V+/PI+) shows the late apoptotic cells, the lower right (quadrant 3, annexin V+/PI-) corresponds to the early apoptotic cells, and the lower left (quadrant 4, annexin V-/PI-) shows viable cells. (B) The rate of apoptosis as quantified by flow cytometry. Values are expressed as the mean ± SD from triplicate experiments. **$p<0.01$ indicates significant differences compared with the control group, #$p<0.05$ and ##$p<0.01$ indicate significant differences compared with the ox-LDL 100 mg/L group.

scope, and photographs were obtained (DMI4000B; Leica, Wetzlar, Germany). In addition, the cells were collected, and DCF fluorescence intensities were analyzed using a FACSAria flow cytometer, with excitation at 488 nm and emission at 525 nm. The data were analyzed using FlowJo software (FlowJo LLC). The experiments were repeated three times.

Immunofluorescence analysis

Cells were seeded onto 48-well plates and fixed with 4% PFA for 30 min at room temperature, permeabilized with 0.5% Triton X-100, blocked with 1% BSA and incubated with rabbit anti-LOX-1 antibody (1:200) overnight at 4°C to analyze LOX-1 expression in the treated RAW264.7 cells. After the cells were washed, they were incubated with a TRITC-conjugated goat anti-rabbit IgG (H+L) antibody (1:200) for 1 h at 37°C. The nuclei were stained with 4',6-diamidino-2-phenylindole (DAPI; Sigma). Fluorescent images were acquired using a fluorescence microscope (DMI4000B; Leica).

Western blot analysis

After the previous treatment, the culture medium was removed. The cells were then placed on ice, washed with ice-

cold PBS, and lysed in RIPA lysis buffer for 30 min. Lysates were clarified by centrifugation at 12,000 rpm for 15 min at 4°C, and the protein concentration in the supernatant was determined with a bicinchoninic acid (BCA) kit (Beyotime Biotech.). Proteins were denatured at 95°C for 5 min in sample buffer containing SDS and β-mercaptoethanol. The samples were subjected to electrophoresis on 10% or 12% SDS-polyacrylamide gels for 50 min at 70 V followed by 100 min at 100 V and then transferred onto nitrocellulose transfer membrane (PALL, New York, NY, USA) sheets for 120 min at 250 mA. These membranes were then blocked with 5% non-fat dry milk (except for membranes used in the analysis of phosphorylated myosin phosphatase targeting protein, where 5% BSA was used for blocking) in Tris-buffered saline containing Tween-20 for 1 h, and incubated with the appropriate primary antibody (β-actin, p38 MAPK, p-p38 MAPK, Bcl-2, Bax, cleaved caspase-3 and LOX-1) at the dilutions recommended by the supplier. Each membrane was then washed before incubation
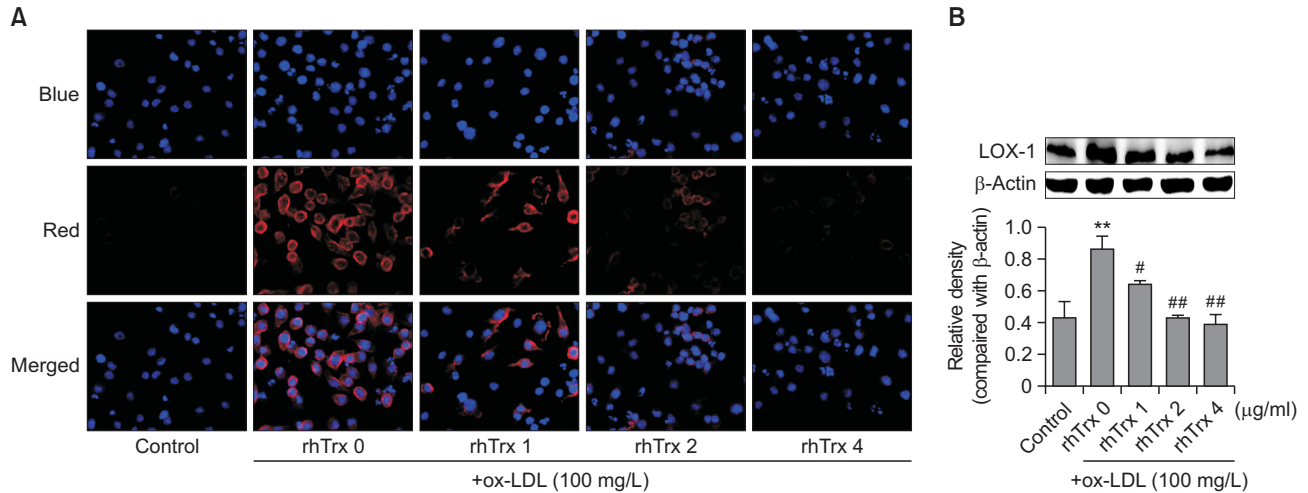
Fig. 3. RhTrx down-regulates ox-LDL-induced LOX-1 expression in RAW264.7 cells. Cells were treated as described in Fig. 1. (A) Immunofluorescence images of LOX-1 (red) and the nucleus (blue) (200×). (B) A representative western blot result (upper panel) and quantitative data (lower panel) of the protein level of LOX-1. β-actin was used as a loading control. Values represent the mean ± SD from three independent experiments. **$p < 0.01$ indicates significant differences from the control group, #$p < 0.05$ and ##$p < 0.01$ indicate significant differences from the ox-LDL 100 mg/L group.
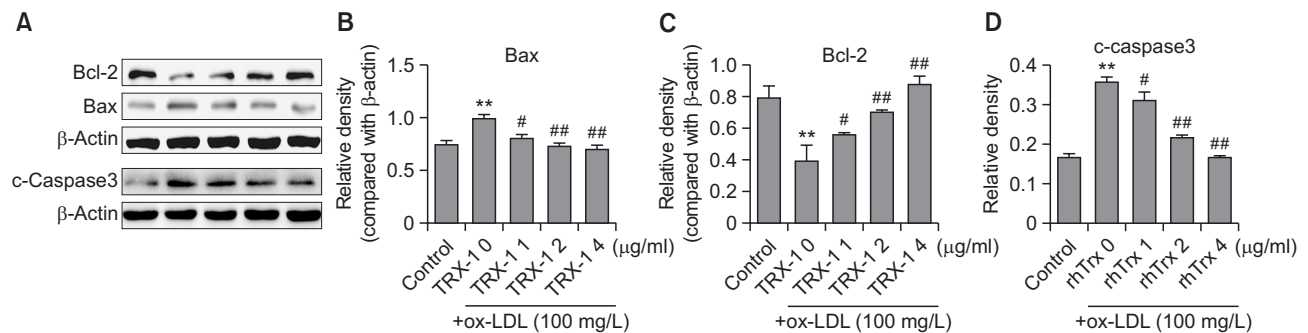

Fig. 4. RhTrx regulates the expression of apoptosis-related proteins in RAW264.7 cells induced by ox-LDL. Cells were treated as described in Fig. 1. (A) Representative western blots show that ox-LDL induced the expression of Bcl-2, Bax and cleaved caspase-3 in RAW264.7 cells that were pretreated with and without rhTrx. (B) Densitometric analysis of Bcl-2 expression. (C) Densitometric analysis of Bax expression. (D) Quantitative analysis of the effect of rhTrx on ox-LDL-induced caspase-3 activation. Values represent the mean ± SD from triplicate experiments.**$p < 0.01$ indicates significant differences compared with the control group, #$p < 0.05$ and ##$p < 0.01$ indicate significant differences compared with the ox-LDL 100 mg/L group.

with a secondary antibody conjugated to horseradish peroxidase for 1 h at room temperature. The blots were visualized using the Electro-Chemi-Luminescence (ECL) detection system with BeyoECL Plus (Beyotime Institute of Biotechnology). The resulting bands were analyzed densitometrically using ImageQuant software (Molecular Dynamics, Sunnyvale, CA).

Statistical analysis

All data were analyzed with GraphPad Prism 5.0 software (GraphPad Software, San Diego, CA, USA) and are expressed as the mean ± SD. Statistical analyses were performed using one-way ANOVA, followed by Tukey's post-hoc test. Differences with $p < 0.05$ were considered statistically significant.

RESULTS

Effect of rhTrx on foam cell formation in RAW264.7 cells

The uptake of ox-LDL by macrophages can trigger foam cell formation and promote the development of atherosclerosis. We evaluated the effect of rhTrx on foam cell formation in RAW264.7 macrophages by oil red O staining and cholesterol content measurement. After exposure to ox-LDL, a significant number of lipid droplets accumulated, and the cellular cholesterol levels and foam cell formation increased in RAW264.7 macrophages (Fig. 1, $p < 0.01$). When the cells were pretreated with rhTrx, both the ox-LDL-induced lipid droplet accumulation and increased cellular cholesterol levels were markedly decreased in RAW264.7 cells in a dose-dependent manner ($p < 0.05$ or $p < 0.01$). Thus, rhTrx inhibits ox-LDL-induced foam cell formation in RAW264.7 cells.
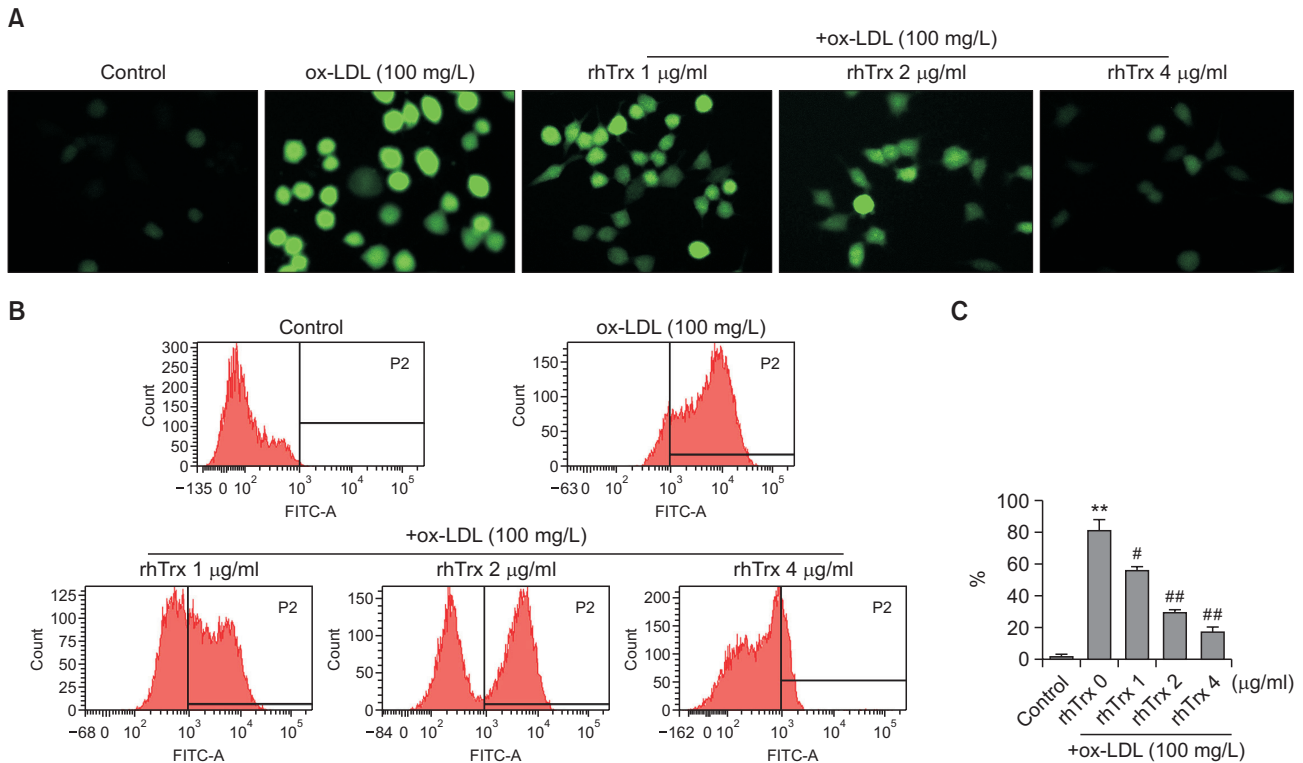
A

B

C

Fig. 5. RhTrx suppresses ox-LDL-induced ROS overproduction in RAW264.7 cells. Cells were pretreated with rhTrx for 30 min prior to ox-LDL exposure for 2 h. ROS were detected using a DCFH-DA probe. (A) Representative fluorescence images show ROS levels in RAW264.7 cells under different treatment conditions. (B) Representative FACS analysis by flow cytometry. (C) Quantitative analysis of the ratio of DCF-DA probe positive cells indicating intracellular ROS production. Values are expressed as the mean ± SD from triplicate experiments. **$p < 0.01$ indicates significant differences compared with the control group, #$p < 0.05$ and ##$p < 0.01$ indicate significant differences compared with the ox-LDL 100 mg/L group.

Effect of rhTrx on ox-LDL-induced apoptosis in RAW264.7 cells

Dual annexin-V-FITC/propidium iodide staining and flow cytometry (FCM) were performed to investigate the effects of rhTrx on ox-LDL-induced apoptosis. Compared with the control, ox-LDL increased the total apoptosis rate from 6.2 ± 2.1% to 47.5 ± 2.4% (Fig. 2, $p < 0.01$). However, pretreatment with rhTrx (1, 2 and 4 μg/mL) significantly reduced apoptosis (34.7 ± 2.7% vs. 47.5 ± 2.4%, $p < 0.01$; 24.7 ± 2.1% vs. 47.5 ± 2.4%, $p < 0.01$; and 17.4 ± 1.1% vs. 47.5 ± 2.4%, $p < 0.01$, respectively) in a concentration-dependent manner.

RhTrx inhibits the ox-LDL-induced up-regulation of LOX-1 expression

In this study, we investigated the effect of rhTrx on ox-LDL-induced LOX-1 up-regulation in RAW264.7 cell by immunofluorescence and western blotting. LOX-1 expression was significantly increased in the ox-LDL group compared with the control group ($p < 0.01$). Pretreatment of the cells with rhTrx (1, 2 and 4 μg/mL) suppressed this ox-LDL-induced up-regulation of LOX-1 expression in a dose-dependent manner ($p < 0.05$ or $p < 0.01$) (Fig. 3).

Effect of rhTrx on ox-LDL-induced Bcl-2, Bax and activated caspase-3 expression

To further demonstrate the contribution of rhTrx to ox-LDL-induced cell apoptosis, we assessed the protein levels of Bcl-2, Bax, and activated caspase-3. The ox-LDL treatment significantly decreased Bcl-2 expression (Fig. 4A, 4B, $p < 0.01$) but increased Bax (Fig. 4A, 4C, $p < 0.01$) and activated caspase-3 expression (Fig. 4A, 4D, $p < 0.01$) in the cultured RAW 264.7 cells compared with the controls. In contrast, pretreatment of the cells with rhTrx increased the expression of Bcl-2 and simultaneously decreased Bax and activated caspase-3 expression (Fig. 4, $p < 0.05$ or $p < 0.01$).

Suppression of ox-LDL-induced ROS production by rhTrx

Oxidative stress plays a vital role in ox-LDL-induced cell injury. In this study, ROS levels in the treated cells were measured. As shown in Fig. 5, ox-LDL significantly increased the ROS levels compared with the control group ($p < 0.01$). Pre-incubation with rhTrx reversed the ox-LDL-induced increase in the ROS levels and induced a visible decrease in the ROS levels ($p < 0.01$).

Effect of rhTrx on ox-LDL-stimulated activation of the p38 MAPK signaling pathway

We detected the level of phosphorylated p38 MAPK by Western blotting to further explore the mechanism underlying the effects of rhTrx on ox-LDL-induced RAW264.7 cell injury. The ox-LDL treatment markedly increased p38 MAPK phosphorylation, whereas pretreatment with rhTrx significantly reduced ox-LDL-induced p38 MAPK phosphorylation (Fig. 6A, $p < 0.01$). Next, we used anisomycin and SB203580 to further
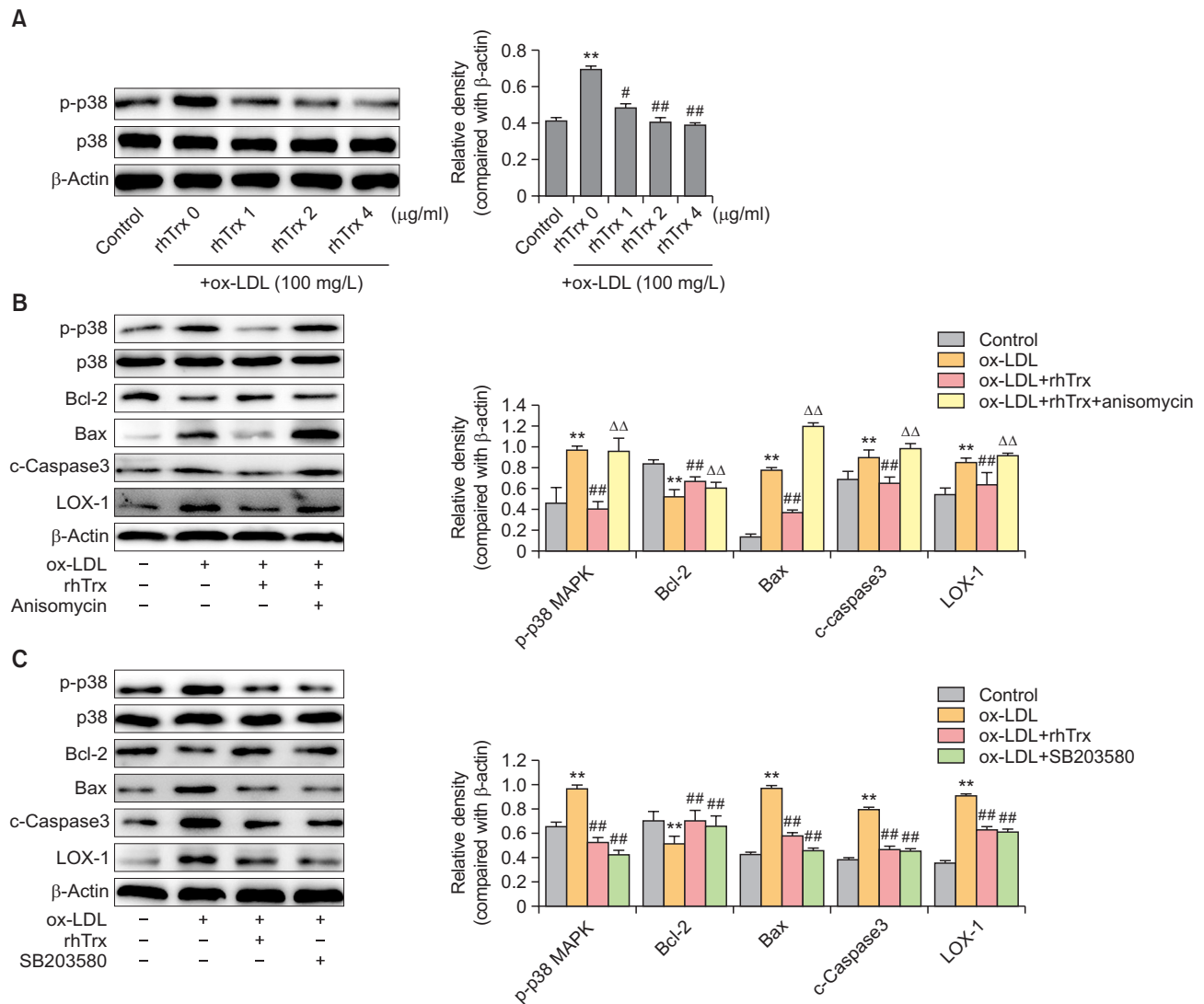
A

B

C

Fig. 6. RhTrx protects RAW264.7 cells from ox-LDL-induced foam cell formation and apoptosis via the p38 MAPK signaling pathway. (A) RAW264.7 cells were pretreated with rhTrx (0, 1, 2, 4 μg/mL) for 20 min prior to ox-LDL treatment (100 mg/L). After 24 h, the expression of total and phosphorylated p38 MAPK was detected by immunoblot assays (left panel) and quantitatively analyzed (right panel). (B) RAW264.7 cells were pretreated with anisomycin (25 μg/mL) for 30 min and then treated with rhTrx before ox-LDL exposure. The expression levels of total and phosphorylated p38 MAPK, apoptosis-related proteins (Bcl-2, Bax and c-caspase3) and LOX-1 were detected by immunoblot assays (left panel) and quantitatively analyzed (right panel). (C) RAW264.7 cells were pretreated with rhTrx (4 μg/mL) or SB203580 (10 μM) and then exposed to ox-LDL. The expressions of total and phosphorylated p38 MAPK, apoptosis-related proteins (Bcl-2, Bax and c-caspase3) and LOX-1 were detected by immunoblot assays (left panel) and quantitatively analyzed (right panel). Values are expressed as the mean ± SD from triplicate experiments. **$p < 0.01$ indicates significant differences from the control group, #$p < 0.05$ and ##$p < 0.01$ indicate significant differences compared with the ox-LDL 100 mg/L group. ΔΔ$p < 0.01$ indicates significant differences compared with the ox-LDL + rhTrx group.

elucidate the signaling mechanism underlying the cytoprotective effect of rhTrx against ox-LDL-induced injury. When cells were pretreated with the p38 MAPK activator anisomycin for 30 min prior to treatment with rhTrx and ox-LDL, the level of phosphorylated p38 MAPK increased, and the effect induced by rhTrx was abolished. The expression of LOX-1 and the pro-apoptotic proteins Bax and cleaved caspase-3 was increased, whereas the expression of the anti-apoptotic protein Bcl-2 was significantly inhibited (Fig. 6B, $p < 0.01$). Additionally, pretreatment with the p38 MAPK antagonist SB203580 before ox-LDL exposure yielded similar effects to rhTrx (Fig. 6C, $p < 0.01$). Al-

together, these results indicate that rhTrx may exert its protective effect on ox-LDL-induced RAW264.7 macrophage injury by inhibiting the activation of the p38 MAPK signaling pathway.

DISCUSSION

Apoptosis of lipid-containing macrophages in advanced atherosclerotic lesions promotes lesional necrosis and results in plaque vulnerability, rupture and acute vascular events (Tabas, 2010; Moore and Tabas, 2011). Thus, inhibition of macro-

phage foam cell formation and apoptosis may be an effective strategy for the prevention and treatment of acute athero-thrombotic vascular events.

In the present study, we demonstrated for the first time that rhTrx dramatically alleviated macrophage-derived foam cell formation and down-regulated LOX-1 expression. In addition, rhTrx reduced the rate of ox-LDL-induced apoptosis, up-regulated the expression of the anti-apoptotic protein Bcl-2 and down-regulated the expression of the pro-apoptotic proteins Bax and cleaved caspase-3. However, the beneficial effects of rhTrx on RAW264.7 macrophage-derived foam cells were abolished by a p38 MAPK activator, indicating that the protective effects of rhTrx were mediated at least in part by suppressing p38 MAPK activation.

The Trx system, which includes Trx, TrxR and NADPH, plays an important role in preserving physiological cardiovascular function and protecting cells from oxidative injury under various pathologic conditions (Yamawaki et al., 2003). A Trx deficiency, which increases the ROS levels and apoptosis, promoted embryonic lethality in mice (Matsui et al., 1996). The addition of rhTrx protected various cell types from oxidant-induced apoptosis, including neurons (Wang et al., 2015), cardiomyocytes (Tao et al., 2006), and liver cells (Cohen et al., 2009), suggesting that Trx may have clinical applications in diseases in which apoptosis plays a pathogenic role. However, whether rhTrx could suppress ox-LDL-induced macrophage injury was unknown. Our present results showed that rhTrx significantly restrained ox-LDL-induced lipid accumulation and macrophage apoptosis by inhibiting ROS generation and p38 MAPK activation.

LOX-1 is a class E scavenger receptor that plays an important role in the uptake of ox-LDL by macrophages (Schaeffer et al., 2009). LOX-1 is a membrane glycoprotein comprised of 273 amino acid residues organized into an N-terminal cytoplasmic domain, a transmembrane domain, an extracellular stalk region, and a C-type lectin-like extracellular domain (Dunn et al., 2008). Basal LOX-1 expression is low, but it is markedly up-regulated by proatherogenic stimuli in vascular cells (Yoshimoto et al., 2011). LOX-1 levels were up-regulated in human carotid-plaque macrophages (Kataoka et al., 1999). Genetic deletion of LOX-1 in LDL receptor-deficient mice decreased atherosclerosis (Mehta et al., 2007), whereas the overexpression of LOX-1 led to advanced disease (Inoue et al., 2005). Over the past decade, down-regulation of LOX-1 expression has been shown to significantly inhibit ox-LDL-induced macrophage foam cell formation and atherosclerosis (Xia et al., 2015). Consistent with these findings, our results showed that rhTrx suppressed LOX-1 expression and foam cell formation induced by ox-LDL in RAW264.7 cells.

Macrophage apoptosis promotes the development of the necrotic core, which is a critical factor that increases the susceptibility to plaque rupture and acute luminal thrombosis (Seimon and Tabas, 2009). Several lines of evidence have shown that oxysterols, the apoptotic component of ox-LDL, induce apoptosis through the mitochondrial pathway. Activation of the mitochondrial apoptosis pathway is regulated by Bcl family members, including anti-apoptotic (Bcl-2 and Bcl-xL) and pro-apoptotic (Bax and Bak) proteins (Rusinol et al., 2004). Macrophages exposed to oxysterols exhibited Bax activation and Bcl-2 down-regulation. However, Bax knockdown substantially attenuated oxysterol-induced macrophage apoptosis (Rusinol et al., 2004). Moreover, ox-LDL-induced macro-
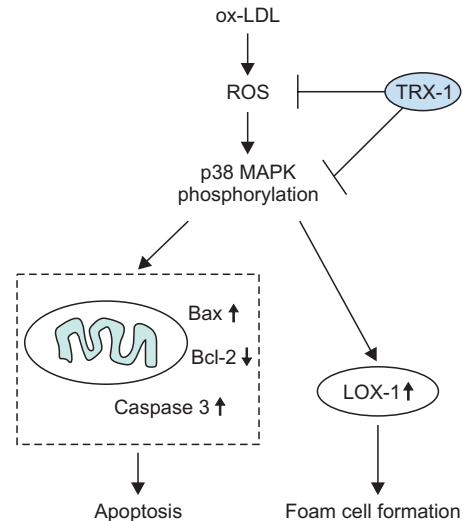

Fig. 7. Proposed molecular mechanisms underlying the effect of rhTrx on ox-LDL-induced foam cell formation and apoptosis in RAW264.7 cells. The uptake of ox-LDL initiates a downstream signal cascade. It promotes ROS overproduction and p38 MAPK phosphorylation. The activation of p38 MAPK signaling could up-regulate Bax expression and down-regulate Bcl-2 and activated caspase-3 expression, which play critical roles in macrophage apoptosis. Moreover, p38 MAPK phosphorylation could up-regulate the expression of LOX-1, a scavenger receptor for ox-LDL, stimulate ox-LDL uptake and promote foam cell formation. RhTrx reduces the production of ROS and suppresses the activation of p38 MAPK induced by ox-LDL, restoring the related pathway and consequently suppressing foam cell formation and apoptosis.

phage apoptosis is suppressed by the down-regulation of Bax and up-regulation of Bcl-2 (Guo et al., 2014). In this study, we observed a significant increase in the expression of Bax and a decrease in the expression of Bcl-2 in ox-LDL-treated macrophages. Pretreatment with rhTrx attenuated the increase in Bax expression and increased Bcl-2 levels. Additionally, caspase-3 is one of the major activated cysteine proteases in the caspase family and is pivotal in cell apoptosis. Activated caspase-3 induces DNA fragmentation and other morphological changes consistent with cell death (Janicke et al., 1998). We examined caspase-3 activity and showed that rhTrx obviously inhibited ox-LDL-induced caspase-3 activation, thus confirming the cytoprotective effects of rhTrx on ox-LDL-induced apoptosis.

In the present study, we found that rhTrx markedly reduced foam cell formation and apoptosis following ox-LDL exposure. As shown in recent studies, ox-LDL induces intracellular lipid deposition and macrophage apoptosis by promoting ROS production (Luo et al., 2015). Trx has been reported to act as a potent scavenger of ROS. In vitro and in vivo studies have demonstrated that Trx has a protective effect against ROS-induced cellular damage. Our results indicated that exposure of RAW264.7 cells to ox-LDL markedly increased intracellular ROS levels, and rhTrx inhibited ox-LDL-induced ROS generation. RhTrx, therefore, protects RAW264.7 macrophages against ox-LDL-induced injury, at least in part, by inhibiting ROS generation.

In addition to serving as a ROS scavenger, Trx, a physiological inhibitor of ASK-1, interacts with the N-terminal portion of ASK1 (Saitoh et al., 1998), the upstream activator of

p38 MAPK pathway, and the Trx-ASK1 complex induces the activity of the p38 MAPK pathway (Hsieh and Papaconstantinou, 2006). Activation of p38 MAPK is associated with LOX-1 expression (Ishiyama *et al*., 2010) and ox-LDL-induced macrophage apoptosis (Wang *et al*., 2013). We investigated the activation of the p38 MAPK signaling pathway to further investigate the mechanisms and signaling pathways underlying the protective effects of rhTrx. In this study, ox-LDL promoted phosphorylation of p38 MAPK, whereas pretreatment with rhTrx inhibited the activation of p38 MAPK signaling. Interestingly, pretreatment with the p38 MAPK activator anisomycin significantly abolished the effects of rhTrx, including inhibition of p38 MAPK phosphorylation, down-regulation of caspase-3 activity and the anti-apoptotic effect. When cells were treated with the p38 MAPK inhibitor SB203850 instead of rhTrx, similar effects to rhTrx were observed. Thus, rhTrx modulates the p38 MAPK signaling pathway in ox-LDL-treated RAW264.7 macrophages, which may be the mechanism underlying the protective effects.

In conclusion (Fig. 7), the results of the present study indicate that rhTrx suppresses foam cell formation and macrophage apoptosis by inhibiting ROS production and the p38 MAPK signaling pathway. These findings provide novel insights into the molecular mechanism of rhTrx and its therapeutic potential in the treatment of atherosclerosis. However, further investigations are required to determine whether rhTrx reduces foam cell formation and apoptosis by inhibiting the p38 MAPK pathway *in vivo*.

ACKNOWLEDGMENTS

REFERENCES

Chen, G., Li, X., Huang, M., Li, M., Zhou, X., Li, Y. and Bai, J. (2016) Thioredoxin-1 increases survival in sepsis by inflammatory response through suppressing endoplasmic reticulum stress. *Shock* **46**, 67-74.

Cohen, J. I., Roychowdhury, S., DiBello, P. M., Jacobsen, D. W. and Nagy, L. E. (2009) Exogenous thioredoxin prevents ethanol-induced oxidative damage and apoptosis in mouse liver. *Hepatology* **49**, 1709-1717.

Cuadrado, A. and Nebreda, A. R. (2010) Mechanisms and functions of p38 MAPK signalling. *Biochem. J.* **429**, 403-417.

D'Annunzio, V., Perez, V., Boveris, A., Gelpi, R. J. and Poderoso, J. J. (2016) Role of thioredoxin-1 in ischemic preconditioning, postconditioning and aged ischemic hearts. *Pharmacol. Res.* **109**, 24-31.

Dai, M. X., Zheng, X. H., Yu, J., Yin, T., Ma, M. J., Zhang, L., Liu, M., Ma, Y., Liu, L. W., Gao, X., Li, Y., Song, L. Q. and Wang, H. C. (2014) The impact of intermittent and repetitive cold stress exposure on endoplasmic reticulum stress and instability of atherosclerotic plaques. *Cell. Physiol. Biochem.* **34**, 393-404.

Dunn, S., Vohra, R. S., Murphy, J. E., Homer-Vanniasinkam, S., Walker, J. H. and Ponnambalam, S. (2008) The lectin-like oxidized low-density-lipoprotein receptor: a pro-inflammatory factor in vascular disease. *Biochem. J.* **409**, 349-355.

Gleissner, C. A. (2016) Translational atherosclerosis research: from experimental models to coronary artery disease in humans. *Atherosclerosis* **248**, 110-116.

Guo, R., Su, Y., Liu, B., Li, S., Zhou, S. and Xu, Y. (2014) Resveratrol suppresses oxidised low-density lipoprotein-induced macrophage apoptosis through inhibition of intracellular reactive oxygen species generation, LOX-1, and the p38 MAPK pathway. *Cell. Physiol. Biochem.* **34**, 603-616.

Holmgren, A. (1985) Thioredoxin. *Annu. Rev. Biochem.* **54**, 237-271.

Hsieh, C. C. and Papaconstantinou, J. (2006) Thioredoxin-ASK1 complex levels regulate ROS-mediated p38 MAPK pathway activity in livers of aged and long-lived Snell dwarf mice. *FASEB J.* **20**, 259-268.

Inoue, K., Arai, Y., Kurihara, H., Kita, T. and Sawamura, T. (2005) Overexpression of lectin-like oxidized low-density lipoprotein receptor-1 induces intramyocardial vasculopathy in apolipoprotein E-null mice. *Circ. Res.* **97**, 176-184.

Ishiyama, J., Taguchi, R., Yamamoto, A. and Murakami, K. (2010) Palmitic acid enhances lectin-like oxidized LDL receptor (LOX-1) expression and promotes uptake of oxidized LDL in macrophage cells. *Atherosclerosis* **209**, 118-124.

Janicke, R. U., Sprengart, M. L., Wati, M. R. and Porter, A. G. (1998) Caspase-3 is required for DNA fragmentation and morphological changes associated with apoptosis. *J. Biol. Chem.* **273**, 9357-9360.

Kamimoto, Y., Sugiyama, T., Kihira, T., Zhang, L., Murabayashi, N., Umekawa, T., Nagao, K., Ma, N., Toyoda, N., Yodoi, J. and Sagawa, N. (2010) Transgenic mice overproducing human thioredoxin-1, an antioxidative and anti-apoptotic protein, prevents diabetic embryopathy. *Diabetologia* **53**, 2046-2055.

Kataoka, H., Kume, N., Miyamoto, S., Minami, M., Moriwaki, H., Murase, T., Sawamura, T., Masaki, T., Hashimoto, N. and Kita, T. (1999) Expression of lectinlike oxidized low-density lipoprotein receptor-1 in human atherosclerotic lesions. *Circulation* **99**, 3110-3117.

Laurent, T. C., Moore, E. C. and Reichard, P. (1964) Enzymatic synthesis of deoxyribonucleotides. IV. Isolation and characterization of thioredoxin, the hydrogen donor from escherichia coli B. *J. Biol. Chem.* **239**, 3436-3444.

Liao, X., Sluimer, J. C., Wang, Y., Subramanian, M., Brown, K., Pattison, J. S., Robbins, J., Martinez, J. and Tabas, I. (2012) Macrophage autophagy plays a protective role in advanced atherosclerosis. *Cell Metab.* **15**, 545-553.

Lin, Y. W., Liu, P. S., Adhikari, N., Hall, J. L. and Wei, L. N. (2015) RIP140 contributes to foam cell formation and atherosclerosis by regulating cholesterol homeostasis in macrophages. *J. Mol. Cell. Cardiol.* **79**, 287-294.

Luo, Y., Sun, G., Dong, X., Wang, M., Qin, M., Yu, Y. and Sun, X. (2015) Isorhamnetin attenuates atherosclerosis by inhibiting macrophage apoptosis via PI3K/AKT activation and HO-1 induction. *PLoS ONE* **10**, e0120259.

Matsui, M., Oshima, M., Oshima, H., Takaku, K., Maruyama, T., Yodoi, J. and Taketo, M. M. (1996) Early embryonic lethality caused by targeted disruption of the mouse thioredoxin gene. *Dev. Biol.* **178**, 179-185.

Mehta, J. L., Sanada, N., Hu, C. P., Chen, J., Dandapat, A., Sugawara, F., Satoh, H., Inoue, K., Kawase, Y., Jishage, K., Suzuki, H., Takeya, M., Schnackenberg, L., Beger, R., Hermonat, P. L., Thomas, M. and Sawamura, T. (2007) Deletion of LOX-1 reduces atherogenesis in LDLR knockout mice fed high cholesterol diet. *Circ. Res.* **100**, 1634-1642.

Moore, K. J., Sheedy, F. J. and Fisher, E. A. (2013) Macrophages in atherosclerosis: a dynamic balance. *Nat. Rev. Immunol.* **13**, 709-721.

Moore, K. J. and Tabas, I. (2011) Macrophages in the pathogenesis of atherosclerosis. *Cell* **145**, 341-355.

Pirillo, A., Norata, G. D. and Catapano, A. L. (2013) LOX-1, OxLDL, and atherosclerosis. *Mediators Inflamm.* **2013**, 152786.

Powis, G. and Montfort, W. R. (2001) Properties and biological activities of thioredoxins. *Annu. Rev. Biophys. Biomol. Struct.* **30**, 421-455.

Rusinol, A. E., Thewke, D., Liu, J., Freeman, N., Panini, S. R. and Sinensky, M. S. (2004) AKT/protein kinase B regulation of BCL family members during oxysterol-induced apoptosis. *J. Biol. Chem.* **279**, 1392-1399.

Saitoh, M., Nishitoh, H., Fujii, M., Takeda, K., Tobiume, K., Sawada, Y., Kawabata, M., Miyazono, K. and Ichijo, H. (1998) Mammalian thioredoxin is a direct inhibitor of apoptosis signal-regulating kinase (ASK) 1. *EMBO J.* **17**, 2596-2606.

Schaeffer, D. F., Riazy, M., Parhar, K. S., Chen, J. H., Duronio, V., Sawamura, T. and Steinbrecher, U. P. (2009) LOX-1 augments oxLDL uptake by lysoPC-stimulated murine macrophages but is not required for oxLDL clearance from plasma. *J. Lipid Res.* **50**, 1676-1684.

Seimon, T. and Tabas, I. (2009) Mechanisms and consequences of macrophage apoptosis in atherosclerosis. *J. Lipid Res.* **50 Suppl**, S382-S387.

Tabas, I. (2009) Macrophage apoptosis in atherosclerosis: consequences on plaque progression and the role of endoplasmic reticulum stress. *Antioxid. Redox Signal.* **11**, 2333-2339.

Tabas, I. (2010) Macrophage death and defective inflammation resolution in atherosclerosis. *Nat. Rev. Immunol.* **10**, 36-46.

Tao, L., Gao, E., Hu, A., Coletti, C., Wang, Y., Christopher, T. A., Lopez, B. L., Koch, W. and Ma, X. L. (2006) Thioredoxin reduces post-ischemic myocardial apoptosis by reducing oxidative/nitrative stress. *Br. J. Pharmacol.* **149**, 311-318.

Wang, B., Tian, S., Wang, J., Han, F., Zhao, L., Wang, R., Ning, W., Chen, W. and Qu, Y. (2015) Intraperitoneal administration of thioredoxin decreases brain damage from ischemic stroke. *Brain Res.* **1615**, 89-97.

Wang, W. L., Meng, Z. X., Zhou, S. J., Li, C. J., Chen, R., Lv, L., Ma, Z. J., Yu, D. M. and Yu, P. (2013) Reduced beta2-glycoprotein I protects macrophages from ox-LDL-induced foam cell formation and cell apoptosis. *Lipids Health Dis.* **12**, 174.

Xia, X., Li, Y., Su, Q., Huang, Z., Shen, Y., Li, W. and Yu, C. (2015) Inhibitory effects of Mycoepoxydiene on macrophage foam cell formation and atherosclerosis in ApoE-deficient mice. *Cell Biosci.* **5**, 23.

Yamawaki, H., Haendeler, J. and Berk, B. C. (2003) Thioredoxin: a key regulator of cardiovascular homeostasis. *Circ. Res.* **93**, 1029-1033.

Yoshimoto, R., Fujita, Y., Kakino, A., Iwamoto, S., Takaya, T. and Sawamura, T. (2011) The discovery of LOX-1, its ligands and clinical significance. *Cardiovasc. Drugs Ther.* **25**, 379-391.